Revisiting the Hydrological Basis of the Budyko Framework With the Hydrologically Similar Groups Principle

Yuchan Chen[1], Xiuzhi Chen[1], Meimei Xue[1], Chuanxun Yang[2,3], Wei Zheng[1], Jun Cao[4], Wenting Yan[1], Wenping Yuan[1]

[1]Guangdong Province Key Laboratory for Climate Change and Natural Disaster Studies, School of Atmospheric Sciences, Sun Yat-sen University, Zhuhai, 519082, China;
[2]Guangzhou Institute of Geochemistry, Chinese Academy of Sciences, Guangzhou, 510640, China;
[3]University of Chinese Academy of Sciences, Beijing, 100049, China;
[4]Guangdong provincial Academy of Environmental Science, Guangzhou, 510635, China;

Correspondence to: Xiuzhi Chen (chenxzh73@mail.sysu.edu.cn)

Abstract. The Budyko framework is a simple and effective tool for estimating the watershed water balance. Quantification of the watershed characteristic-related parameter (Pw) is critical to accurate water balance simulations by using the Budyko framework. However, there is no universal method for calculating the Pw as the interactions between hydrologic, climatic, and watershed characteristic factors differ greatly between watersheds globally. To fill this research gap, this study introduced the hydrologically similar groups principle into the Budyko framework and provided a framework for quantifying the Pw of watersheds in similar environments. We firstly classified the selected 366 watersheds worldwide into six hydrologically similar groups based on watershed attributes, including climate, soil moisture, and vegetation. Results show that soil moisture (SM) and fractional vegetation cover (FVC) are two controlling factors of the Pw in each group . The Pw values in dry watersheds (SM≤20mm) monotonically increase with SM but in humid watersheds (SM>20mm) convert to monotonically decrease with SM, in power functions. And the FVC shows linearly correlated with the Pw values of watersheds in most hydrologically similar groups, except in those with no strong seasonality and moist soils. Then, multiple non-linear regression models between Pw and the controlling factors (SM and FVC) were developed to estimate the Pw for the six hydrologically similar groups individually. Cross-validations using the bootstrap sampling method (R^2 = 0.63) and validations of time-series GRDC runoff data (R^2 = 0.89) both indicate that the proposed models overall present a satisfactory performance of the Pw parameter in the Budyko framework. Overall, this study is a new attempt to quantify the unknown watershed characteristic-related parameter in the Budyko framework using the hydrologically similar groups method. Results will be helpful for improving the applicability of the Budyko framework in estimating annual runoff of watersheds in diverse climates and with different characteristics.

1 Introduction

There has been an increasing interest in estimating the water balance of watersheds with a simple and effective tool — the Budyko framework. Unlike the process-based models that typically require a large number of parameters as inputs for accurate simulations (Caracciolo et al., 2018; Lei et al., 2014), the Budyko framework is a top-down approach relating a catchment's long-term evaporative ratio (ratio between actual evapotranspiration and precipitation) to its aridity index (ratio between potential evapotranspiration and precipitation) and is rooted on a firm physical basis (Vora and Singh, 2021; Sivapalan, 2003; Wang and Tang, 2014). Currently, the Budyko framework has been widely used for assessing linkages and feedbacks between climate forcing and land surface characteristics on water and energy cycles (Zhang et al., 2001; Milly and Shmakin, 2002; Li et al., 2013; Xu et al., 2013), prompting a great deal of empirical, theoretical, and process-based studies (Chen and Sivapalan, 2020; Roderick and Farquhar, 2011; Rau et al., 2018; Goswami and Goyal, 2022).

The original Budyko equation assumes that evapotranspiration is mainly controlled by precipitation (representing the availability of water) and potential evapotranspiration (representing the availability of energy) (Budyko, 1974; Wang et al., 2022). Despite its solid performance, the original Budyko equation still produces a bias between modeled and measured evapotranspiration or runoff because it does not consider the effects of watershed characteristics other than mean annual climatic conditions on water balance (Kim and Chun, 2021; Zhang et al., 2001). As a result, hydrologists have invested considerable efforts to improve model performance by introducing parameters related to watershed characteristics (watershed characteristic parameter, Pw) into the original Budyko equation. The popular parametric equations of the Budyko framework are presented in Table 1.

Table 1. Parametric formulations of the Budyko framework (Pw - watershed characteristic parameter; ET - actual evaporation, R - runoff, P - precipitation, PET - potential evapotranspiration, all in mm yr^{-1}).

Reference	Formulation	Pw (Theoretical range)	Reference values of Pw
Budyko (1974)	$\frac{ET}{P} = \left[\frac{PET}{P}\tanh\left(\frac{PET}{P}\right)^{-1}(1-exp(-\frac{PET}{P}))\right]^{0.5}$	0.5	0.5
Zhang et al. (2001)	$\frac{ET}{P} = \frac{1+w\frac{PET}{P}}{1+w\frac{PET}{P}+(\frac{PET}{P})^{-1}}$	w $(0, \infty)$	Trees – 2.0, Plants – 0.5

Turc (1954), Mezentsev (1955), Choudhury (1999), Yang et al. (2008)	$\frac{ET}{P}=\frac{1}{\left[1+(\frac{P}{PET})^{n}\right]^{\frac{1}{n}}}$	n $(0,\infty)$	Field – 2.6, River basins – 1.8
Wang and Tang (2014)	$\frac{ET}{P}=\frac{1+\frac{PET}{P}-\sqrt{(1+\frac{PET}{P})^{2}-4\varepsilon(2-\varepsilon)\frac{PET}{P}}}{2\varepsilon(2-\varepsilon)}$	ε (0,1)	0.55 - 0.58
Tixeront (1964), Fu (1981), Zhou et al. (2015a)	$\frac{R}{P}=\left[1+\left(\frac{P}{PET}\right)^{-m}\right]^{\frac{1}{m}}-(\frac{P}{PET})^{-1}$	m $(1,\infty)$	Forest – 2.83, Shrub – 2.33, Grassland or cropland – 2.28, Mixed land – 2.12

From the hydrological point of view, the Pw controls the fraction of precipitation diverted into the runoff for a given aridity index (Caracciolo et al., 2018). Watersheds with larger Pw values convert larger parts of precipitation to evapotranspiration and consequently less part to runoff than those with smaller Pw values; and some studies defined the Pw as the water retention capacities of watersheds (Fu, 1981; Zhou et al., 2015a). Overall, the Pw denotes the adjustment of water-energy partitioning by watershed characteristics (Yao et al., 2017; Li et al., 2013).

During the past decades, researchers have done lots of work to quantify the Pw for the accurate simulation of evapotranspiration or runoff using the Budyko framework (Wang et al., 2022; Yao et al., 2017; Guo et al., 2019; Yu et al., 2021) and made considerable contributions for improving the estimation of Pw by taking into account the influences from watershed characteristics (Fu, 1981; Liu and Liang, 2015; Guan et al., 2022; Yang et al., 2008). Although there is agreement that the Pw represents the integrated effects of various environmental factors (Wang et al., 2022; Liu et al., 2022b; Yu et al., 2021; Gan et al., 2021), studies still differed greatly as to what factors and effects should relate to the Pw and failed to give a general framework for quantifying the Pw. For instance, whether the Pw in the Budyko framework is controlled by vegetation or not has been much debated. Ning et al. (2017) found that the Pw generally had a positive correlation with vegetation coverage. Zhang et al. (2018) obtained the sensitivity of the Pw to changes in LAI by taking a derivative of the Pw function with respect to LAI, implying a crucial role of vegetation cover in impacting the Pw. However, some other studies indicated that most regions or watersheds show no significant influences of vegetation indices or coverage on Pw (Li et al., 2013; Liu et al., 2021). For example, Li et al. (2013) pointed out the variations in the Pw values are not entirely controlled by vegetation coverage in the small catchments. Another study from Liu et al. (2021) also found a weak correlation between the vegetation leaf area index and the Pw. Therefore, more in-depth studies are in need for revisiting the hydrological Basis of Pw in the Budyko Framework.

Here, we hypothesize that watersheds with similar climatic, hydrologic, and watershed-related characteristics have consistent controlling factors of Pw in the Budyko Framework. But, to date, very few researches have been conducted on classifying watersheds based on the highly variable climate-Pw relationships in the Budyko framework. This may be an important reason why there is disagreement among researchers about the factors and extent of influence on Pw.

To fill the research gap, this study proposed a classification method of watersheds using the hydrologically similar groups principle and then developed a framework for estimating the Pw (PwM) separately for different watersheds in hydrologically similar groups to simulate global runoff. We expect that classifying watersheds into hydrologically similar groups is useful for exploring the effect of watershed characteristics on its water balance and interpreting the physical meaning of the Pw in the Budyko framework. Overall, 726 records of hydrological data in 366 watersheds from globally published datasets were collected for analyses (Supplement 1). These 366 watersheds were classified into six hydrologically similar groups according to the hydrologically homogenous attributes of watersheds using the Decision Tree Regressor method. Then, we identified the controlling factors of the Pw from various environmental factors in each hydrologically similar group and developed multiple non-linear regression models for estimating the Pw in the Budyko framework. This study highlights the need to account for the interactions among hydrologic, climatic, and watershed characteristic factors for explaining the Pw in the Budyko framework.

2 Fu's formula

This study employed the Fu's formula (Zhou et al., 2015a) to analyze Pw in the Budyko framework. Among the parametric equations, Fu's equation has received the most application and turned out to be a more generalized form (Zhou et al., 2015a). The formula is expressed as:

$$\frac{R}{P} = \left(1 + \left(\frac{P}{PET}\right)^{-Pw}\right)^{\frac{1}{Pw}} - \left(\frac{P}{PET}\right)^{-1} \quad (1)$$

where R/P is a dimensionless annual water yield coefficient; P/PET is an aridity index; and Pw is a dimensionless constant varying from 1 to infinity, and represents water retention capacity for evapotranspiration. When Pw=1, all the precipitation would become flow and the residence time is 0. When Pw→infinity, all precipitation would remain in the watershed and residence time would equal the time for all precipitation conversion to evapotranspiration. So, the natural watersheds with a large Pw value may be "non-conservative" (i.e., precipitation is not the sum of streamflow and evapotranspiration), because part of the water remain in the watershed may come from groundwater flow and other hardly or not measurable

flows. To be more cautious, in this study, the empirical upper limit for Pw was 10 to ensure that the watersheds in question were conservative.

3 Data

3.1 Hydrological data

Hydrological data for modeling, including runoff (R, mm yr^{-1}) and corresponding precipitation (P, mm yr^{-1}), were collected from globally published datasets (726 samples listed in Supplement 1, Fig. 1). Potential evapotranspiration (PET, mm yr^{-1}) data were downloaded from version 4.05 of the CRU TS (Climatic Research Unit gridded Time Series) climate dataset (https://doi.org/10.6084/m9.figshare.11980500), which is produced by the CRU at the University of East Anglia. For consistency, we used PET values extracted from the CRU TS dataset of all watersheds listed in Supplement 1, even for studies with PET values reported. The PET values were extracted based on the coordinate points of watersheds. Using collected and extracted the R, P and PET data, we calculated the R/P and P/PET for each site. Then, we derived the Pw values according to Equation 1.

Observed river discharge data for validation were obtained from the Global Runoff Data Centre (GRDC, https://www.bafg.de/GRDC/EN/02_srvcs/21_tmsrs/riverdischarge_node.html). Only the GRDC stations meeting the following criteria were selected for further analysis: (1) The sites with continuous time-series runoff observations during the period 2000–2016 and corresponding surface soil moisture, fractional vegetation cover and seasonal index data were also available during such a period; (2) The drainage area reports can be found in the original data to provide area parameters for converting original flow volumes to runoff rates; (3) The geographical coordinates reports can be found in the original data and the shape of the drainage can be found in the GRDC Watershed Boundaries (2011); (4) The watersheds of "non-conservative" ($m>10$) and unrealistic runoff rates ($m<1$) are removed. Based on these criteria, 545 GRDC stations were selected for validation (Fig. 1). Then, the flow volumes of selected sites were converted to runoff rates (Ghiggi et al., 2019).

We used the boundary of watersheds provided by GRDC Watershed Boundaries (2011) to extract the average values of PET and P from grid datasets for each watershed. The PET values were extracted from the CRU TS dataset. The P values for runoff reconstruction were extracted from Global Precipitation Climatology Centre (GPCC) Precipitation Total Full V2018 (0.5×0.5) data provided by the NOAA/OAR/ESRL PSL, Boulder, Colorado, USA. It is because that the Global Precipitation Climatology Centre (GPCC) precipitation data was found to be more agreeable with the observation in the

previous research compared to the CRU TS precipitation dataset(Ahmed et al., 2019; Degefu et al., 2022; Fiedler and Döll, 2007; Hu et al., 2018; Salaudeen et al., 2021).

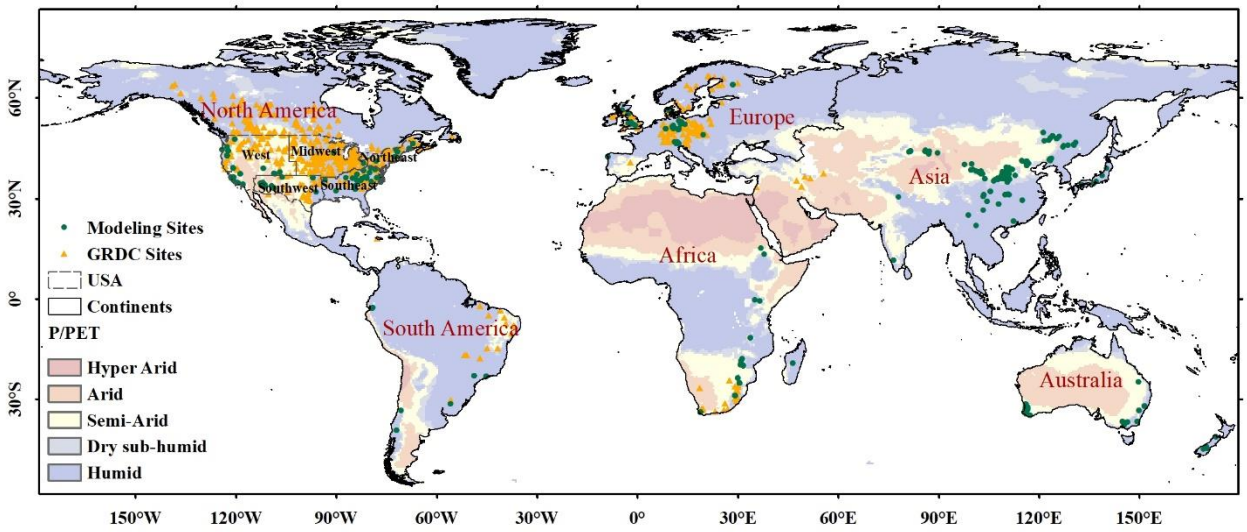

Figure 1. Location of the observation sites for modeling (green dots) (n = 726) and the GRDC (Global Runoff Data Centre) observation sites (orange triangles) (n = 545) for validation. Background colors represent UNEP (1997) climate classification for P/PET values (Hyper Arid: P/PET<0.03; Arid: 0.03≤P/PET<0.2; Semi-Arid: 0.2≤P/PET<0.5; Dry sub-humid: 0.5≤P/PET<0.65; Humid: P/PET≥0.65). The globe was divided into nine geographic regions: North America (west, southwest, midwest, northeast, southeast, except of the USA), South America, Africa, and Europe.

3.2 Watershed characteristic-related data

The watershed characteristic-related factors mainly include surface soil moisture (0-10cm underground, SM), fractional vegetation cover (FVC) and seasonal index (SI) of Walsh and Lawler (1981). For the GRDC watersheds, records of these three fields were extracted from grid data based on the boundary files provided by GRDC Watershed Boundaries (2011). For the collected watersheds from published literatures without boundary files, data of these three fields were extracted from grid data according to the coordinate points of these watersheds. The sources of datasets are summarized in Table 2.

Table 2. Data sources for watershed characteristic factors

Watershed characteristic factors	Data source/version	Units	Reference
Surface soil moisture (0-10cm underground, SM)	GLDAS Noah Land Surface Model L4	mm	Rodell et al. (2004)
Fractional vegetation cover (FVC)	GLASS FVC V4	m^2 m^{-2}	Liang et al. (2021)
Seasonal index (SI)	CRU TS dataset version 4.03, global maps of seasonality indices	dimensionless	Walsh and Lawler (1981);Feng (2019)

4 Methods

4.1 Classification of watersheds into hydrologically similar groups using watershed attributes

A hydrologically similar group (hydrologically homogeneous region) is defined as a group of drainage basins whose hydrologic responses are similar (Kanishka and Eldho, 2020). Therefore, the relationship between Pw and the watershed characteristic variable does not change substantially in a hydrologically similar group. However, when that relationship between Pw and the variable changes as certain boundaries are crossed, the corresponding watersheds are divided into different groups by these boundaries.

Three watershed characteristic variables — surface soil moisture (SM), rainfall seasonality index (SI), and fractional vegetation cover (FVC) — were selected for classification. For SM and FVC, the bounded intervals of the variables were given by the Decision Tree Regressor (DTR). The locations of splits in DTR were used as dividing intervals. The Scikit-learn library (Pedregosa et al., 2011) in Python provides the DTR used in this study. The criterion for measuring the quality of the split was set to "poisson" which uses reduction in Poisson deviance to find splits. The "random" strategy was used to choose local optimal splitting at each node. The results and performances of DTR are shown in Supplement 2. Based on the criteria used by Walsh and Lawler (1981), we divided the SI into three parts ($SI \leq 0.4$, $0.4 < SI \leq 0.8$, $SI > 0.8$) to represent three hydroclimatic seasonality (precipitation spread throughout the year, marked seasonality with a short drier season, extreme seasonality with a long drier season). Finally, six hydrologically similar groups were classified (Table 3).

Table 3. Classification of watersheds

Soil moisture classifier	Water soil regime	Seasonality index classifier	Seasonality precipitation regime	Fractional vegetation cover classifier	vegetation cover regime	Name of the group
$SM \leq 20$	Dry soil	——	——	——	——	IN_D
$SM > 20$	Wet soil	$SI \leq 0.4$	Seasonless	——	——	IN_{WP}
		$0.4 < SI \leq 0.8$	Marked seasonality	$FVC \leq 0.2$ $0.2 < FVC \leq 0.5$ $FVC > 0.5$	Low density Middle density High density	IN_{WMS} IN_{WMM} IN_{WML}
		$SI > 0.8$	Extreme seasonality	——		IN_{WE}

4.2 Setup of proposed Pw simulation model (PwM)

4.2.1 PwM with the classification of hydrologically similar groups

We performed regression analysis between the Pw and watershed characteristic variables to determine the input variables of the PwM. The variables whose R^2 of the regression model was greater than 0.1 were selected as input variables. We used a polynomial as the basic model form. Each term of the polynomial depends on the regression model of the corresponding variable and the Pw. For each hydrological group, the PwM is modeled as a function as,

$$Pw = \sum Coef\_n \times f(Var\_n) \quad (2)$$

where *Pw* represents the value of the Pw; *Var_n* represents the input variable that pass the regression test; *f* corresponds to the function derived from the regression of *Pw* on *Var_n*; *Coef_n* represents the empirical coefficient fitted by multiple non-linear regression (MNR).

4.2.2 PwM without classification of hydrologically similar groups

For comparison, we estimated Pw without the hydrologically similar groups, defined as non_PwM. The non_PwM is as follows,

$$non\_Pw = a_1 \times SM^2 + a_2 \times SM + b_1 \times FVC^2 + b_2 \times FVC \quad (3)$$

where *non_Pw* is the annual value of Pw simulated by *non_PwM*; *SM* is annual average value of surface soil moisture (0-10cm underground); *FVC* is annual average value of fractional vegetation cover; a_1, a_2, b_1 and b_2 represent the empirical coefficient fitted by least square method.

4.3 Model validation

4.3.1 Performance metrics

Three performance metrics were used to assess the accuracy of the PwM. The term N is the number of observations, i is the i^{th} value to be simulated, and y_s and y_o are the simulated and observed series, respectively.

The relative bias (RelBIAS) represents systematic errors. A positive value indicates a general overestimation, while a negative one indicates an underestimation. The perfect agreement is achieved when RelBIAS equals to zero. RelBIAS is defined as:

$$RelBIAS = \frac{mean(y_s - y_o)}{mean(y_o)} \quad (4)$$

The coefficient of determination (R^2) assesses the linear relationship between the simulated and observed time series data. It is defined as:

$$R^2 = \frac{\sum_{i=1}^{N}(y_o^i - \bar{y}_o)(y_s^i - \bar{y}_s)}{[\sum_{i=1}^{N}(y_o^i - \bar{y}_o)^2]^{0.5}[\sum_{i=1}^{N}(y_s^i - \bar{y}_s)^2]^{0.5}} \quad (5)$$

The Nash–Sutcliffe efficiency (NSE) (Nash and Sutcliffe, 1970), a goodness-of-fit index, is usually used to assess the accuracy of the model. When NSE = 1, the model predictions perfectly match the observed data. A value higher than 0 indicates that the modeled mean is a good predictor compared to the observed value. It is defined as:

$$NSE = 1 - \frac{\sum_{i=1}^{N}(y_s^i - y_o^i)^2}{\sum_{i=1}^{N}(y_o^i - \bar{y}_o)^2} \quad (6)$$

4.3.2 Cross-validations using the bootstrap sampling method

We used cross-validation to test the stability of the proposed PwM using the bootstrap sampling method. The collected public data were split into two parts, one for model training and the other for model validation. A subset of 60% of the data was randomly selected using the bootstrap sampling method for training PwM. The remaining 40% of the data was used to evaluate the model performance using the validation metrics in section 4.3.1. For each metric, the term N is the number of test sets, i is the i^{th} value to be simulated by the trained PwM, and y_s and y_o are the simulated and observed series of test sets, respectively. The process was repeated randomly 10000 times. We documented the cross-validation result of each bootstrapping and showed them in the violin plot (Fig. 3).

4.3.3 Validations of GRDC time-series runoff reconstruction results

To further assess the model performance, we applied the proposed PwM into Fu's model to reconstruct the time-series runoff data of GRDC from 2000 to 2016. Finally, the time-series runoff data from 545 GRDC stations, which were selected by Sect. 3.1, were used to evaluate the model performance using the validation metrics in section 4.3.1. For each metric, the terms y_s and y_o represent the simulated and observed time-series runoff data, respectively.

5 Results

5.1 The new proposed model for estimating Pw in Fu's formula

The regressions between Pw in Fu's formula and watershed characteristic variables collected from globally published datasets are shown in Fig. 2. Analyses show that soil moisture (SM) and fractional vegetation cover (FVC) are strongly

correlated to Pw in each group. The Pw values in dry watersheds with SM≤20mm monotonically increase with SM following a power function (Fig. 2a). However, in humid watersheds with SM>20mm, the Pw values convert to monotonically decrease with SM, which is also in a power function (Fig. 2b). And the fractional vegetation cover (FVC) shows linearly correlated with the Pw values of watersheds in most hydrologically similar groups but differ greatly between different groups (Fig. 2c-h). There is positive linear correlation between Pw and FVC in the IN_D, IN_{WMS} and IN_{WE} groups; while the relationship turns to be a negative linear equation in the IN_{WMM} and IN_{WML} groups. However, in the IN_{WP} group, the relationship between Pw and FVC is not significant. Therefore, in the proposed PwM, SM and FVC were selected as input variables (i.e., *Var_n*) for all the groups, except that FVC was rejected in the IN_{WP} group. The formula in PwM for calculating the Pw is modeled as sum of a power function of SM and a linear function of FVC, given by Equation 7.

$$\boldsymbol{Pw} = \begin{cases} \mathbf{0.91} \times \boldsymbol{SM}^{\mathbf{0.38}} + \mathbf{1.48} \times \boldsymbol{FVC} & (IN_D, SM \le 20) \\ \mathbf{28.72} \times \boldsymbol{SM}^{\mathbf{-0.76}} & (IN_{WP}, SM > 20, SI \le 0.4) \\ \mathbf{39.03} \times \boldsymbol{SM}^{\mathbf{-0.96}} + \mathbf{11.82} \times \boldsymbol{FVC} & (IN_{WMS}, SM > 20, 0.4 < SI \le 0.8, FVC \le 0.2) \\ \mathbf{33.76} \times \boldsymbol{SM}^{\mathbf{-0.71}} - \mathbf{1.47} \times \boldsymbol{FVC} & (IN_{WMM}, SM > 20, 0.4 < SI \le 0.8, 0.2 < FVC \le 0.5) \\ \mathbf{20.41} \times \boldsymbol{SM}^{\mathbf{-0.42}} - \mathbf{4.221} \times \boldsymbol{FVC} & (IN_{WML}, SM > 20, 0.4 < SI \le 0.8, FVC > 0.5) \\ \mathbf{3078} \times \boldsymbol{SM}^{\mathbf{-2.43}} + \mathbf{3.53} \times \boldsymbol{FVC} & (IN_{WE}, SM > 20, SI > 0.8) \end{cases} \quad (7)$$

where Pw is the annual value of Pw; *SM* is annual average value of surface soil moisture (0-10cm underground); *FVC* is annual average value of fractional vegetation cover.

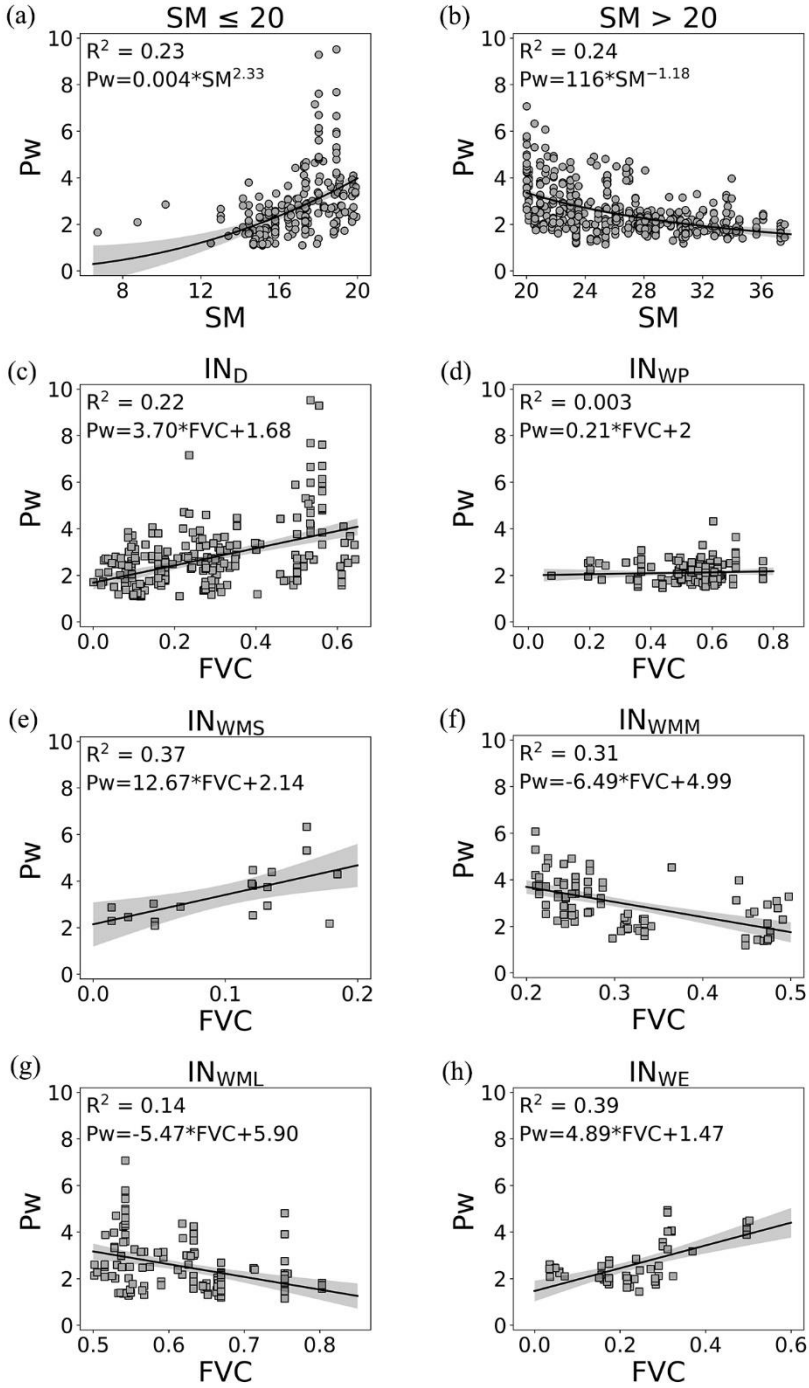

Figure 2. Regression between Pw in Fu's formula and (a) SM (SM≤20mm), (b)SM (SM>20mm), (c)FVC (IN_D), (d)FVC (IN_{WP}), (e)FVC (IN_{WMS}), (f)FVC (IN_{WMM}), (g)FVC (IN_{WML}), and (h)FVC (IN_{WE}). Symbol shapes indicate SM (dot) and FVC (square).

5.2 Cross-validations based on data collected from globally published literatures

The performance of the PwM and non_PwM were cross-validated based on the data collected from globally published literatures using the bootstrap sampling method (Fig. 3). On average, the ensemble RelBIAS of the Pw simulated by the PwM is slightly negative (Fig. 3a), indicating a weak tendency to underestimate the values of Pw, but the maximum relative

bias is less than 0.1. The interquartile range of R^2 for the PwM is from 0.35 to 0.40, with a median of 0.37. The scores of R^2 are higher than 0.3 in more than 95% of the bootstrap sampling events. The NSE skill scores show that in most bootstrap samplings, the estimation error estimated variance for the PwM is less than the variance of the observations (NSE > 0), with the interquartile range from 0.33 to 0.39. In comparison, the maximum relative bias of the Pw simulated by the non_PwM is 0.12, the median of R^2 is 0.13, and the median of NSE is 0.13. Overall, cross-validations show that the performance of the PwM with the hydrologically similar groups is better and more stable than that of the non_PwM.

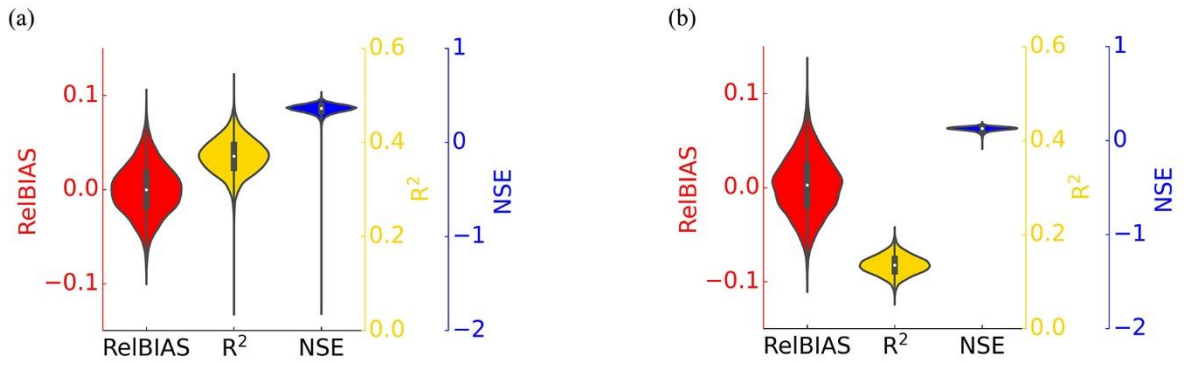

Figure 3. Cross-validation results of (a) PwM and (b) non_PwM. A violin represents the distribution of the considered skill scores. The white dot on the violin plot represents the median. The black bar in the center of the violin represents the interquartile range. Colors distinguish three performance metrics: Red (RelBIAS), yellow (R^2) and blue (NSE).

The skill scores of cross-validations for the six groups are shown in Fig. 4, respectively. Though the overall RelBIAS of the PwM is negative, the PwM tends to overestimate values of Pw in the IN_{WP} group (the median of RelBIAS is positive). The IN_{WMS} group scores highest in R^2, with a median of 0.73, and the lowest in the IN_{WP} group with a median of 0.16. The grouped NSE scores show more uncertainty than the overall, especially in the IN_{WMS}: the lower adjacent value (LAV) larger than zero indicates more skill than the mean of observations, however, the outliers are far below zero. The low NSE value may be due to the low number of watersheds sampled in this interval, which increased the inconclusive results.

Figure 5 showed the simulated R/P by the PwM in compassion to site observations. The R^2 between the observed and the simulated values is 0.63 (Fig. 5a). The model performs well in humid regions with P/PET≥1 at southeast America, Europe, middle China and southeast of Australia. However, the PwM likely underestimated the runoff in the arid (P/PET<0.2) and semi-arid regions (0.2≤P/PET<0.5), which mainly occurred in western America and northwest China (Fig. 5b).

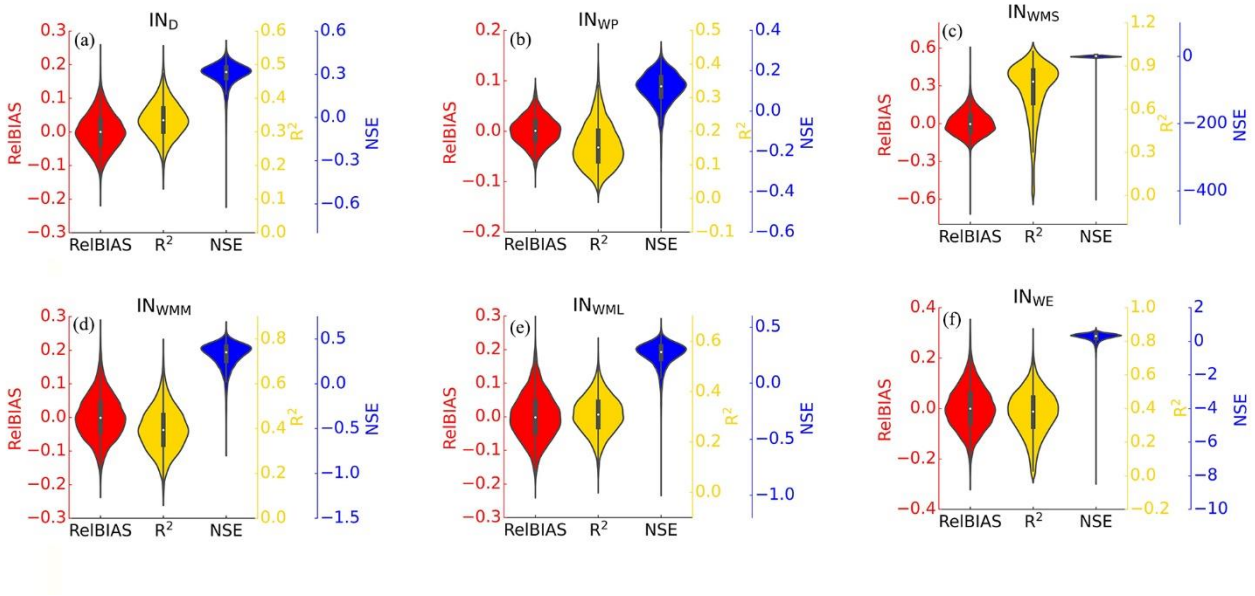

Figure 4. Cross-validation results of PwM for (a) IN_D, (b) IN_{WP}, (c) IN_{WMS}, (d) IN_{WMM}, (e) IN_{WML}, and (f) IN_{WE}.

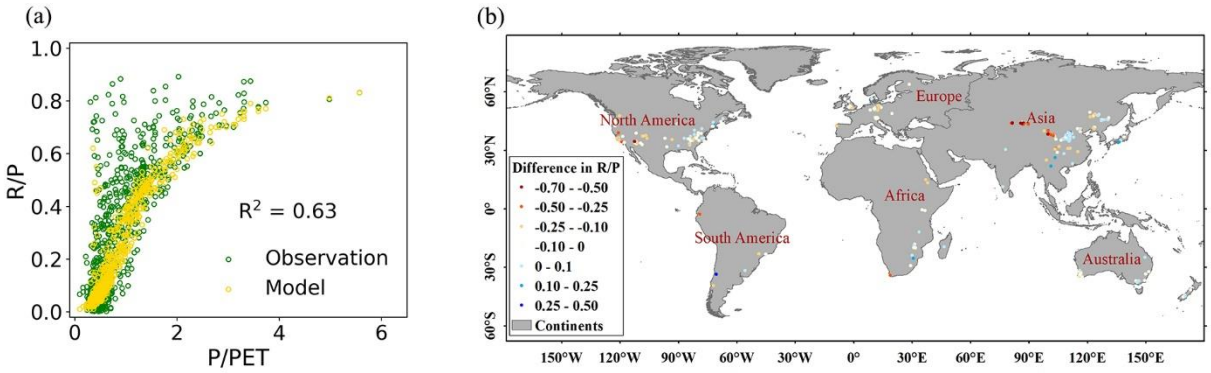

Figure 5. Simulated R/P using PwM in comparison with the observations collected from published literatures. (a) Scatter plots between R/P (yellow: simulation; green: observations) and P/PET; (b) Difference between simulated R/P from the PmM and observations from the published datasets.

5.3 Validations of reconstructing the time-series GRDC runoff

For the selected 545 GRDC watersheds, the annual runoff estimated by the PwM ranges from 229.84 to 320.34 mm, which is slightly lower than the observed range of GRDC (265.82 ~ 345.50 mm yr^{-1}) (Fig. 6a). Overall, the temporal evolution of runoff is captured well in the period 2000-2010. However, since 2011, the consistency between reconstructed runoff and GRDC runoff decreases, and the reconstruction results are constantly lower than the GRDC observations. The scatter plot between simulated and observed R/P also shows a slight underestimation of reconstructed global long-term mean runoff (Fig. 6b). The spatial patterns of long-term mean runoff reconstruction are shown in Fig. 6c-f. The estimated time-series runoff shows lower values in the west of the United States and south

of Africa, and show higher values in the northeastern United States and the European Mediterranean area, in comparison with the GRDC time-series.

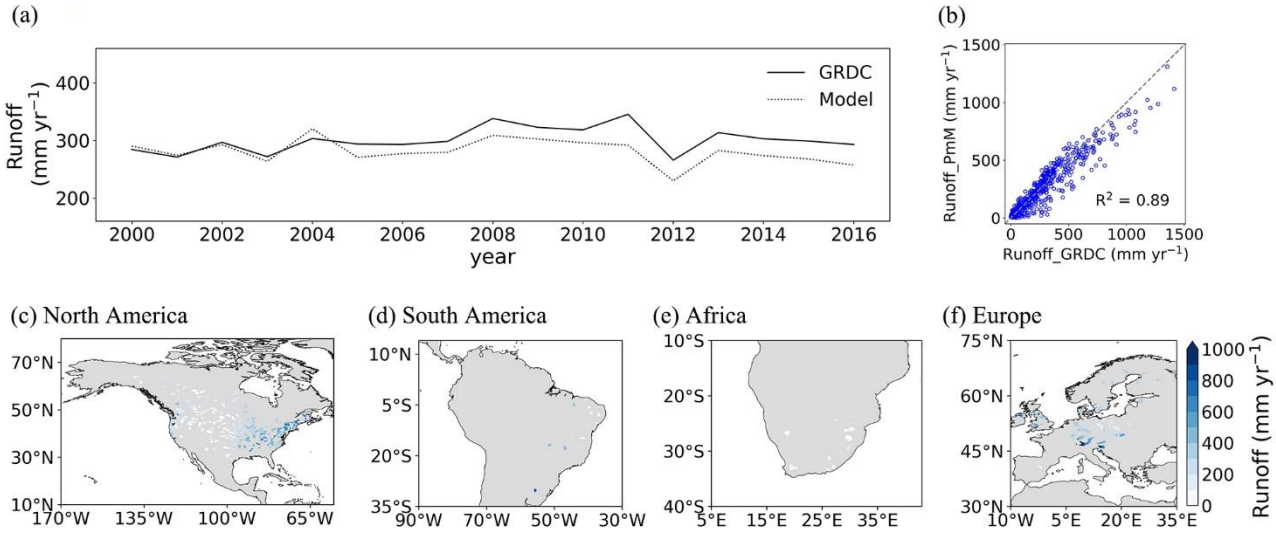

Figure 6. Time-series runoff reconstruction results in the selected GRDC stations. (a) Time-series annual mean runoff of the selected 545 GRDC watersheds; (b) Scatterplot between the modeled runoff and observed runoff; The spatial distribution of annual mean runoff in (c) North America, (d) South America, (e) Africa, and (f) Europe.

Figure 7 displays the skill scores of the reconstructed runoff by the PwM in comparison with the GRDC ensemble from 2000-2016. It can be seen that the result of reconstruction by PwM, in general, is satisfactory, as indicated by the RelBIAS close to 0. The underestimation of runoff mainly occurs in the high mountains of the western United States (Fig. 7a), when the runoff is much smaller.. Humid regions such as the northeastern United States and the European Mediterranean area have quite high R^2 values, while lower values are observed in the semi-arid ($0.2 \leq P/PET < 0.5$) and the dry sub-humid ($0.5 \leq P/PET < 0.65$) regions, which are mainly located in the western and midwestern United States (Fig. 7e-h). There is low NSE scores in the watersheds where runoff is unusually under-estimated or over-estimated (Fig. 7i-l), especially in the western United States.

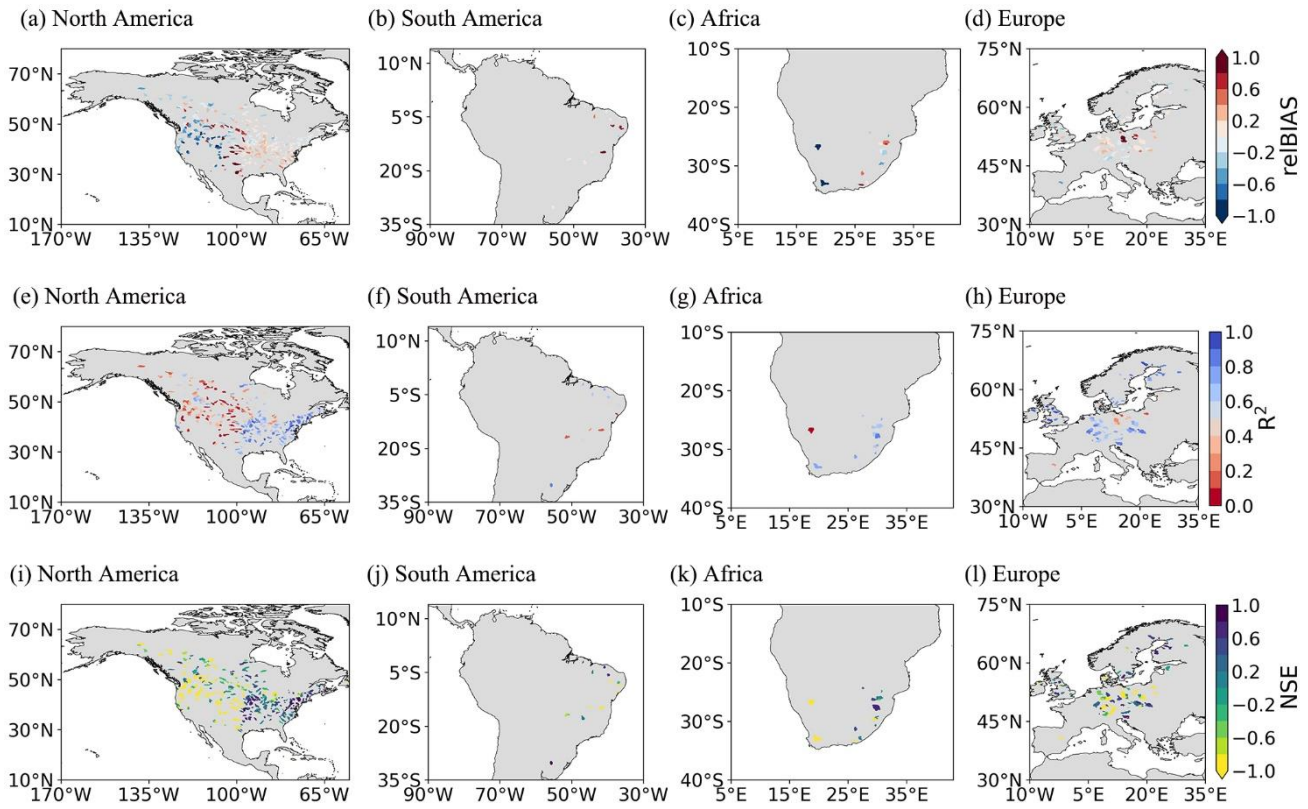

Figure 7. Spatial distribution of the skill scores of the reconstructed time-series runoff.

We classified the GRDC data into nine geographic regions (Fig. 1) and further evaluated the performance of PwM in each sub-region individually. In general, the simulated time-series runoff is consistent with the time-series observations (Fig. 8-9), except in the western United States, where runoff was consistently underestimated (Fig. 8a). Spatially, there is an underestimation of runoff in sub-regions like the western United States (Fig. 8a) and high latitudes in North America (Fig. 8f). The runoff underestimation is more severe in the arid areas in the western United States (Fig. 9a) than in the relatively wet areas in the northwest of North America (Fig. 9f). The reconstructed time-series runoff in the Milk River watershed (GRDC station number: 4220501) and Near Lethbridge watershed (GRDC station number: 4213111) both show an underestimation of annual runoff in the arid areas. The Milk River and the Near Lethbridge are two adjacent watersheds with similar drainage areas located on the border of the United States and Canada. However, the underestimation is more serious in Milk River watershed (RelBIAS=-0.32, annual mean P/PET=0.52) than in the Near Lethbridge watershed (RelBIAS=-0.27, annual mean P/PET=0.55). Interestingly, the spatial pattern of runoff underestimation almost coincides with that of glaciers. Therefore, we considered that glacial meltwater might be the probable causation of runoff underestimation in glacier-covered areas (Li et al., 2021), where glacial snowmelt plays a more important role as a water input in arid regions than in wet ones. Therefore, the underestimation of runoff in the western United States is greater than

in the northwest of North America. Temporally, runoff is mostly underestimated by PwM in the year 2011, when the world experienced abnormal high temperatures (Frölicher et al., 2018; NOAANCEI, 2011)and glacier melting was thus accelerated to bring an increase in runoff yielding (Du et al., 2022; Liu et al., 2022a).

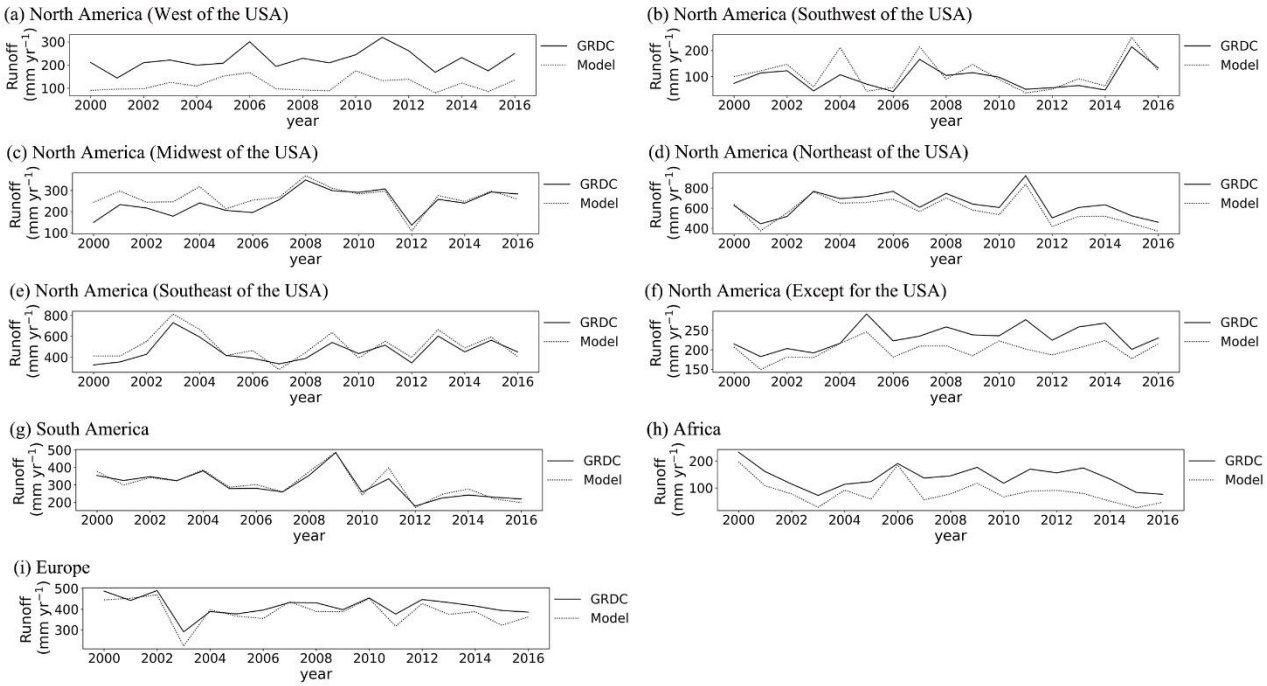

Figure 8. Observed time-series runoff versus reconstructed time-series runoff. Nine geographic sub-regions were in Fig. 1: North America ((a) west, (b) southwest, (c) midwest, (d) northeast, (e) southeast, (f) except of the USA), (g) South America, (h) Africa, and (i) Europe.

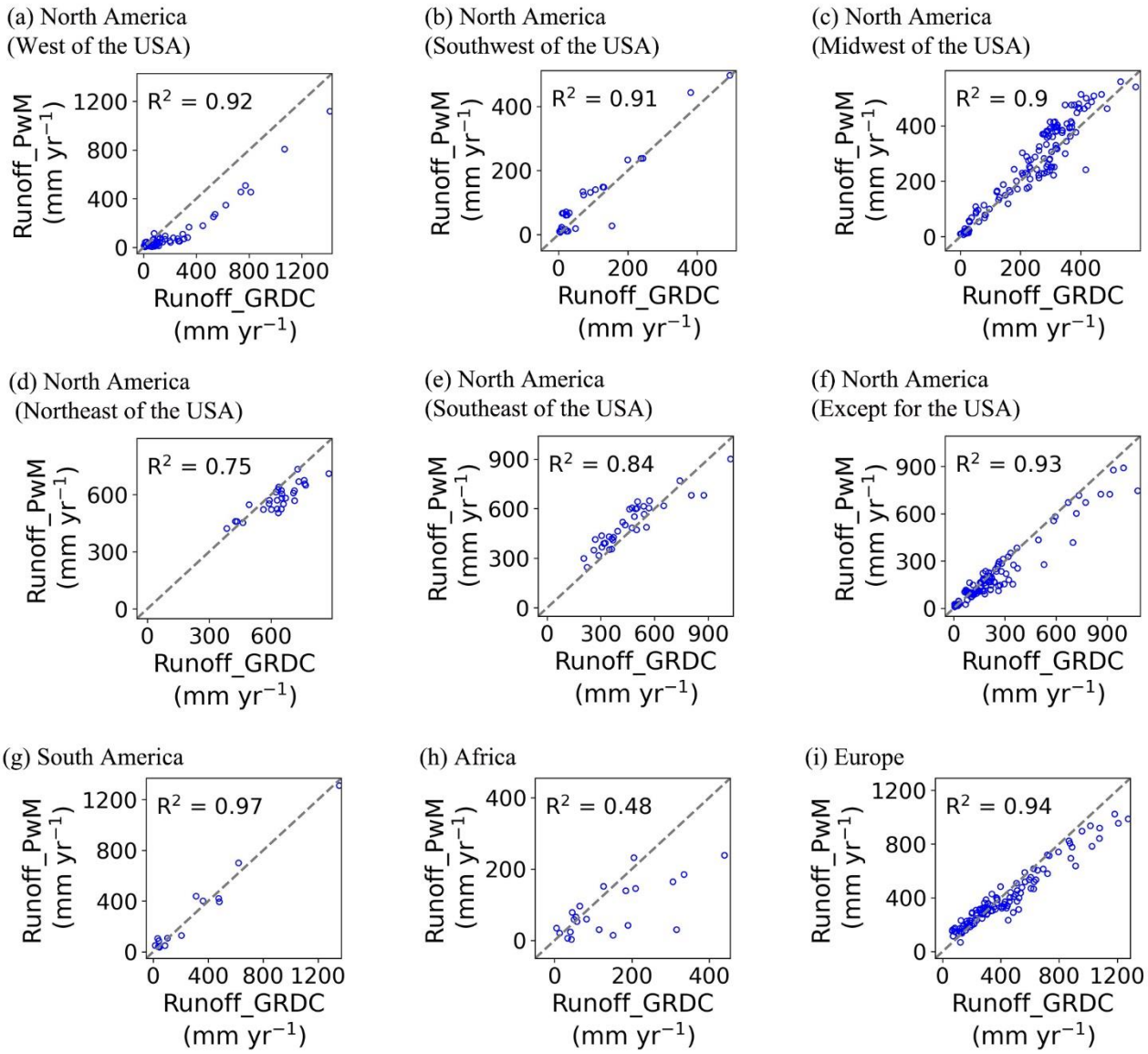

Figure 9. Scatterplots between observed annual mean runoff and reconstructed annual mean runoff. Nine geographic sub-regions were in Fig. 1: North America ((a) west, (b) southwest, (c) midwest, (d) northeast, (e) southeast, (f) except of the USA), (g) South America, (h) Africa, and (i) Europe.

6 Discussion

Zhou et al. (2015a) provided a Budyko equation derived from Fu's equation and confirmed that this is a valid framework for studying hydrological responses. However, the physical meaning of the Pw in the Budyko equation has remained unknown (Greve et al., 2015; Reaver et al., 2022; Zhou et al., 2015b; Zhang et al., 2004). In this paper, we selected the new Fu's equation and developed a universal framework for estimating Pw. Our results show that, to a large extent, the Pw in Budyko equation can be well estimated by the PwM using only soil moisture and fractional vegetation

cover parameters. This indicates that soil moisture and fractional vegetation cover strongly control the water balance of watersheds (Gan et al., 2021; Chen and Sivapalan, 2020; Yang et al., 2009; Wang et al., 2021).

The new proposed framework for calculating the Pw in the Budyko equation is built on empirically-based power function of soil moisture and a linear function of fractional vegetation cover (Equation 7). Our findings are consistent with those of Chen and Sivapalan (2020), which also indicated the power relationship between Pw and soil moisture. The important finding here is that there is a critical soil moisture threshold at 20 mm (Fig.2) to classify the watersheds with two different water balances. The Pw values in dry watersheds (SM≤20mm) monotonically increases with SM but in humid watersheds (SM>20mm) converts to monotonically decrease with SM, in power functions . The probable reason is that transpiration usually increases as soil water increases in a relative dry condition (Jiao et al., 2019; Bierhuizen, 1958; Wang et al., 2012; Yao et al., 2016; Schwarzel et al., 2020). However, once the soil moisture exceeds the threshold, like 20 mm in this study, the acceleration of transpiration from soil moisture slows down quickly (Havranek and Benecke, 1978; Verhoef and Egea, 2014; Metselaar and De Jong Van Lier, 2007). These findings are highly in line with previous studies (Havranek and Benecke, 1978; Jiao et al., 2019; Cavanaugh et al., 2011; Ducharne et al., 1998), although the threshold of soil moisture varied slightly between these studies, e.g., 0.25 $m^3 m^{-3}$ in Ducharne et al. (1998), 0.10 $m^3 m^{-3}$ in Cavanaugh et al. (2011) and 0.20 $m^3 m^{-3}$ in Jiao et al. (2019), respectively.

This study confirms a close linear relationship between Pw and fractional vegetation cover, similar as those reported in previous studies (Ning et al., 2017; Zhang et al., 2018; Xu et al., 2013). For example, Li et al. (2013) found that the spatial pattern of the Pw was linearly correlated with the spatial pattern of the vegetation cover fraction. However, previous similar findings were mostly reported in large watersheds or non-humid watersheds (Li et al., 2013; Gan et al., 2021). For those small and wet watersheds, vegetation-related factors were considered to be weakly correlated with the watershed characteristic parameter of the Budyko framework (Liu et al., 2021; Padrón et al., 2017; Yang et al., 2014). The classifications of watersheds into different hydrological similarity groups in this study provide new insights for explaining this confusion. In dry watersheds (IN_D), the relationship between Pw and fractional vegetation cover followed a positive linear function (Fig. 2c). This finding was consistent with the majority view that vegetation transpiration increases (reflected by the increased Pw) with increasing vegetation coverage in regions with insufficient soil moisture (Wang et al., 2012; Yao et al., 2016; Schwarzel et al., 2020). In wet watersheds, the relationship between Pw and fractional vegetation cover is not only affected by the SI seasonality, but is also restricted by the background value of fractional vegetation cover itself. This is typical obvious in wet watersheds with marked SI seasonality (0.4<SI≤0.8). Despite having similar seasonal

conditions, the Pw values in the watersheds with low-density vegetation coverage (FVC≤0.2) monotonically increase with FVC (Fig. 2e). However, the Pw values in the watersheds with middle-density (0.2<FVC≤0.5, Fig. 2f) and the high-density (FVC>0.5, Fig. 2g) vegetation coverage monotonically decrease with FVC. This confirms that climate, soil moisture, and vegetation coverage are not independent factors affecting the water balance, and the physiological characteristics of vegetation greatly depend on climate and soil moisture (Gan et al., 2021; Yang et al., 2009). When vegetation was coupled with other catchment properties, the watershed characteristic parameter exhibited greater variations (Gan et al., 2021). Therefore, the classification of watersheds is crucial and supports the hypothesis that watersheds in the same class would function similarly in environments with similar climate, soil moisture, and vegetation characteristics (Kanishka and Eldho, 2017; Sinha et al., 2019).

Although the overall performance of PwM was satisfactory, we noted that the accuracy of the runoff simulated by the Budyko framework in some regions show either an overestimation or an underestimation. It is because the Pw in our study is only forced with soil moisture, seasonality index and fractional vegetation cover, and thus the estimated runoff could not clearly account for impacts from other drivers, like the effects of temperature anomalies and glacial meltwater on the hydrological regimes (Liu et al., 2022b). This is probably one of the main reasons for the severe underestimation of runoff in western North America and southern Europe (Fig. 7a, d). Future in-depth researches are in need to examine influences from other impact factors to improve the accuracy of Pw estimation in the Budyko framework.

7 Conclusions

This study developed a new framework for estimating the Pw in the Budyko framework for watersheds in similar environments based on the hydrologically similar groups principle. Generally, the proposed method not only represented the runoff observations in 366 watersheds from global published literatures, but could also reconstruct the time-series runoff in 545 GRDC stations. Moreover, the findings indicated that the Pw is closely related to soil moisture and fractional vegetation cover, and the relationship varies across specific hydrologic similarity groups. However, due to the complexity of hydrological processes, the new framework could not fully account for the impacts from all other factors, which might result in an underestimation of runoff in regions with glaciers or under climate with temperature anomalies. Overall, our findings lay a sound basis for estimating the Pw in the Budyko framework, provide references for calibrating the hydrological models, and will be helpful for improving global runoff estimations.

Code availability. The pieces of code that were used for all analyses are available from the authors upon request.

Data availability. All data used in this study are publicly available. PET data are available from CRU TS (https://doi.org/10.6084/m9.figshare.11980500), SM data are available from GLDAS (https://disc.gsfc.nasa.gov/datasets/GLDAS_NOAH025_M_2.1/summary?keywords=GLDAS), FVC data are available from GLASS (http://www.glass.umd.edu/05D/FVC/), SI data are available from HydroShare (http://www.hydroshare.org/resource/ff287c90c9e947a78e351c8d07d9d3f3), P data used to model validation are available from GPCC (https://psl.noaa.gov/data/gridded/data.gpcc.html), and observed river discharge data are available from GRDC (https://www.bafg.de/GRDC/EN/02_srvcs/21_tmsrs/riverdischarge_node.html).

Author contributions. XC designed the study and proposed the scientific hypothesis. YC implemented the experiments, conducted the analysis and wrote the paper. MX helped with data collection, and checked the technical adequacy of the experiments. CY and WZ helped with data processing. WPY provided the guidance on the seasonal indices (SI). CY, WZ, CJ, WTY and WPY reviewed and edited the manuscript. XC oversaw the study and conducted manuscript revision as a mentor.

Competing interests. The contact author has declared that neither they nor their co-authors have any competing interests.

Financial support. This study was financed by the National Natural Science Foundation of China (grant numbers 31971458, 41971275), Innovation Group Project of Southern Marine Science and Engineering Guangdong Laboratory (Zhuhai), grant number 311021009 and the Special High-level Plan Project of Guangdong Province (grant number 2016TQ03Z354).

References

Ahmed, K., Shahid, S., Wang, X., Nawaz, N., and Khan, N.: Evaluation of gridded precipitation datasets over arid regions of Pakistan, Water, 11, 210, 2019.

Bierhuizen, J.: Some observations on the relation between transpiration and soil moisture, Netherlands Journal of Agricultural Science, 6, 94-98, 1958.

Budyko, M. I.: Climate and life, Academic press1974.

Caracciolo, D., Pumo, D., and Viola, F.: Budyko's based method for annual runoff characterization across different climatic areas: an application to United States, Water Resources Management, 32, 3189-3202, 2018.

Cavanaugh, M. L., Kurc, S. A., and Scott, R. L.: Evapotranspiration partitioning in semiarid shrubland ecosystems: a two-site evaluation of soil moisture control on transpiration, Ecohydrology, 4, 671-681, 2011.

Chen, X. and Sivapalan, M.: Hydrological basis of the Budyko curve: Data-guided exploration of the mediating role of soil moisture, Water Resources Research, 56, e2020WR028221, 2020.

Choudhury, B.: Evaluation of an empirical equation for annual evaporation using field observations and results from a biophysical model, Journal of Hydrology, 216, 99-110, 1999.

Degefu, M. A., Bewket, W., and Amha, Y.: Evaluating performance of 20 global and quasi-global precipitation products in representing drought events in Ethiopia I: Visual and correlation analysis, Weather and Climate Extremes, 35, 100416, 2022.

Du, X., Silwal, G., and Faramarzi, M.: Investigating the impacts of glacier melt on stream temperature in a cold-region watershed: Coupling a glacier melt model with a hydrological model, Journal of Hydrology, 605, 127303, 2022.

Ducharne, A., Laval, K., and Polcher, J.: Sensitivity of the hydrological cycle to the parametrization of soil hydrology in a GCM, Climate dynamics, 14, 307-327, 1998.

Feng, X.: Global maps of seasonality indices, HydroShare [dataset], 2019.

Fiedler, K. and Döll, P.: Global modelling of continental water storage changes–sensitivity to different climate data sets, Advances in Geosciences, 11, 63-68, 2007.

Frölicher, T. L., Fischer, E. M., and Gruber, N.: Marine heatwaves under global warming, Nature, 560, 360-364, 2018.

Fu, B.: On the calculation of the evaporation from land surface, Chinese Journal of Atmospheric Sciences, 5, 23-31, 1981.

Gan, G., Liu, Y., and Sun, G.: Understanding interactions among climate, water, and vegetation with the Budyko framework, Earth-Science Reviews, 212, 103451, 2021.

Ghiggi, G., Humphrey, V., Seneviratne, S. I., and Gudmundsson, L.: GRUN: an observation-based global gridded runoff dataset from 1902 to 2014, Earth System Science Data, 11, 1655-1674, 2019.

Goswami, U. P. and Goyal, M. K.: Relative Contribution of Climate Variables on Long-Term Runoff Using Budyko Framework, in: Water Resources Management and Sustainability, Springer, 147-159, 2022.

GRDC: Watershed Boundaries of GRDC Stations / Global Runoff Data Centre, Federal Institute of Hydrology (BfG) [dataset], 2011.

Greve, P., Gudmundsson, L., Orlowsky, B., and Seneviratne, S. I.: Introducing a probabilistic Budyko framework, Geophysical Research Letters, 42, 2261-2269, 2015.

Guan, X., Zhang, J., Yang, Q., and Wang, G.: Quantifying the effects of climate and watershed structure changes on runoff variations in the Tao River basin by using three different methods under the Budyko framework, Theoretical and Applied Climatology, 1-14, 2022.

Guo, A., Chang, J., Wang, Y., Huang, Q., Guo, Z., and Li, Y.: Uncertainty analysis of water availability assessment through the Budyko framework, Journal of Hydrology, 576, 396-407, 2019.

Havranek, W. M. and Benecke, U.: The influence of soil moisture on water potential, transpiration and photosynthesis of conifer seedlings, Plant and Soil, 49, 91-103, 1978.

Hu, Z., Zhou, Q., Chen, X., Li, J., Li, Q., Chen, D., Liu, W., and Yin, G.: Evaluation of three global gridded precipitation data sets in central Asia based on rain gauge observations, International Journal of Climatology, 38, 3475-3493, 2018.

Jiao, L., Lu, N., Fang, W., Li, Z., Wang, J., and Jin, Z.: Determining the independent impact of soil water on forest transpiration: a case study of a black locust plantation in the Loess Plateau, China, Journal of Hydrology, 572, 671-681, 2019.

Kanishka, G. and Eldho, T.: Watershed classification using isomap technique and hydrometeorological attributes, Journal of Hydrologic Engineering, 22, 04017040, 2017.

Kanishka, G. and Eldho, T.: Streamflow estimation in ungauged basins using watershed classification and regionalization techniques, Journal of Earth System Science, 129, 1-18, 2020.

Kim, D. and Chun, J. A.: Revisiting a Two-Parameter Budyko Equation With the Complementary Evaporation Principle for Proper Consideration of Surface Energy Balance, Water Resources Research, 57, e2021WR030838, 2021.

Lei, H., Yang, D., and Huang, M.: Impacts of climate change and vegetation dynamics on runoff in the mountainous region of the Haihe River basin in the past five decades, Journal of Hydrology, 511, 786-799, 2014.

Li, D., Pan, M., Cong, Z., Zhang, L., and Wood, E.: Vegetation control on water and energy balance within the Budyko framework, Water Resources Research, 49, 969-976, 2013.

Li, Y., Li, F., Shangguan, D., and Ding, Y.: A new global gridded glacier dataset based on the Randolph Glacier Inventory version 6.0, Journal of Glaciology, 67, 773-776, 2021.

Liang, S., Cheng, J., Jia, K., Jiang, B., Liu, Q., Xiao, Z., Yao, Y., Yuan, W., Zhang, X., and Zhao, X.: The global land surface satellite (GLASS) product suite, Bulletin of the American Meteorological Society, 102, E323-E337, 2021.

Liu, J., You, Y., Zhang, Q., and Gu, X.: Attribution of streamflow changes across the globe based on the Budyko framework, Science of The Total Environment, 794, 148662, 2021.

Liu, J., Long, A., Deng, X., Yin, Z., Deng, M., An, Q., Gu, X., Li, S., and Liu, G.: The Impact of Climate Change on Hydrological Processes of the Glacierized Watershed and Projections, Remote Sensing, 14, 1314, 2022a.

Liu, Q. and Liang, L.: Impacts of climate change on the water balance of a large nonhumid natural basin in China, Theoretical and Applied Climatology, 121, 489-497, 2015.

Liu, S., Wang, X., Zhang, L., Kong, W., Gao, H., and Xiao, C.: Effect of glaciers on the annual catchment water balance within Budyko framework, Advances in Climate Change Research, 13, 51-62, 2022b.

Metselaar, K. and de Jong van Lier, Q.: The shape of the transpiration reduction function under plant water stress, Vadose Zone Journal, 6, 124-139, 2007.

Mezentsev, V.: Back to the computation of total evaporation, Meteorologia i Gidrologia, 5, 24-26, 1955.

Milly, P. and Shmakin, A.: Global modeling of land water and energy balances. Part II: Land-characteristic contributions to spatial variability, Journal of Hydrometeorology, 3, 301-310, 2002.

Nash, J. E. and Sutcliffe, J. V.: River flow forecasting through conceptual models part I—A discussion of principles, Journal of hydrology, 10, 282-290, 1970.

Ning, T., Li, Z., and Liu, W.: Vegetation dynamics and climate seasonality jointly control the interannual catchment water balance in the Loess Plateau under the Budyko framework, Hydrology and Earth System Sciences, 21, 1515-1526, 2017.

NOAANCEI: Monthly National Climate Report for July 2011, NOAA National Centers for Environmental Information, 2011.

Padrón, R. S., Gudmundsson, L., Greve, P., and Seneviratne, S. I.: Large-scale controls of the surface water balance over land: Insights from a systematic review and meta-analysis, Water Resources Research, 53, 9659-9678, 2017.

Pedregosa, F., Varoquaux, G., Gramfort, A., Michel, V., Thirion, B., Grisel, O., Blondel, M., Prettenhofer, P., Weiss, R., and Dubourg, V.: Scikit-learn: Machine learning in Python, the Journal of machine Learning research, 12, 2825-2830, 2011.

Rau, P., Bourrel, L., Labat, D., Frappart, F., Ruelland, D., Lavado, W., Dewitte, B., and Felipe, O.: Hydroclimatic change disparity of Peruvian Pacific drainage catchments, Theoretical and applied climatology, 134, 139-153, 2018.

Reaver, N. G., Kaplan, D. A., Klammler, H., and Jawitz, J. W.: Theoretical and empirical evidence against the Budyko catchment trajectory conjecture, Hydrology and Earth System Sciences, 26, 1507-1525, 2022.

Rodell, M., Houser, P., Jambor, U., Gottschalck, J., Mitchell, K., Meng, C.-J., Arsenault, K., Cosgrove, B., Radakovich, J., and Bosilovich, M.: The global land data assimilation system, Bulletin of the American Meteorological society, 85, 381-394, 2004.

Roderick, M. L. and Farquhar, G. D.: A simple framework for relating variations in runoff to variations in climatic conditions and catchment properties, Water Resources Research, 47, 2011.

Salaudeen, A., Ismail, A., Adeogun, B. K., Ajibike, M. A., and Zubairu, I.: Evaluation of ground-based, daily, gridded precipitation products for Upper Benue River basin, Nigeria, Engineering and Applied Science Research, 48, 397-405, 2021.

Schwarzel, K., Zhang, L., Montanarella, L., Wang, Y., and Sun, G.: How afforestation affects the water cycle in drylands: A process-based comparative analysis, Global Change Biology, 26, 944-959, 2020.

Sinha, J., Jha, S., and Goyal, M. K.: Influences of watershed characteristics on long-term annual and intra-annual water balances over India, Journal of Hydrology, 577, 123970, 2019.

Sivapalan, M.: Process complexity at hillslope scale, process simplicity at watershed scale: Is there a connection?, EGS-AGU-EUG Joint Assembly, 7973,

Tixeront, J.: Prediction of streamflow, IAHS publication, 118-126, 1964.

Turc, L.: The water balance of soils. Relation between precipitation, evaporation and flow, Ann. Agron, 5, 491-569, 1954.

UNEP: World atlas of desertification, United Nations Environment Programme [dataset], 1997.

Verhoef, A. and Egea, G.: Modeling plant transpiration under limited soil water: Comparison of different plant and soil hydraulic parameterizations and preliminary implications for their use in land surface models, Agricultural and Forest Meteorology, 191, 22-32, 2014.

Vora, A. and Singh, R.: Satellite based Budyko framework reveals the human imprint on long-term surface water partitioning across India, Journal of Hydrology, 602, 126770, 2021.

Walsh, R. and Lawler, D.: Rainfall seasonality: description, spatial patterns and change through time, Weather, 36, 201-208, 1981.

Wang, D. and Tang, Y.: A one-parameter Budyko model for water balance captures emergent behavior in Darwinian hydrologic models, Geophysical Research Letters, 41, 4569-4577, 2014.

Wang, F., Xia, J., Zou, L., Zhan, C., and Liang, W.: Estimation of time-varying parameter in Budyko framework using long short-term memory network over the Loess Plateau, China, Journal of Hydrology, 607, 127571, 2022.

Wang, H., Lv, X., and Zhang, M.: Sensitivity and attribution analysis of vegetation changes on evapotranspiration with the Budyko framework in the Baiyangdian catchment, China, Ecological Indicators, 120, 106963, 2021.

Wang, Y., Bredemeier, M., Bonell, M., Yu, P., Feger, K.-H., Xiong, W., and Xu, L.: Comparison between a statistical approach and paired catchment study in estimating water yield response to afforestation, Revisiting Experimental Catchment Studies in Forest Hydrology:(Proceedings of a Workshop held during the XXV IUGG General Assembly in Melbourne, June–July 2011, 3-11,

Xu, X., Liu, W., Scanlon, B. R., Zhang, L., and Pan, M.: Local and global factors controlling water-energy balances within the Budyko framework, Geophysical Research Letters, 40, 6123-6129, 2013.

Yang, D., Shao, W., Yeh, P. J. F., Yang, H., Kanae, S., and Oki, T.: Impact of vegetation coverage on regional water balance in the nonhumid regions of China, Water Resources Research, 45, 2009.

Yang, H., Yang, D., Lei, Z., and Sun, F.: New analytical derivation of the mean annual water-energy balance equation, Water resources research, 44, 2008.

Yang, H., Qi, J., Xu, X., Yang, D., and Lv, H.: The regional variation in climate elasticity and climate contribution to runoff across China, Journal of hydrology, 517, 607-616, 2014.

Yao, J., Mao, W., Yang, Q., Xu, X., and Liu, Z.: Annual actual evapotranspiration in inland river catchments of China based on the Budyko framework, Stochastic Environmental Research and Risk Assessment, 31, 1409-1421, 2017.

Yao, W., Xiao, P., Shen, Z., Wang, J., and Jiao, P.: Analysis of the contribution of multiple factors to the recent decrease in discharge and sediment yield in the Yellow River Basin, China, Journal of Geographical Sciences, 26, 1289-1304, 2016.

Yu, K.-x., Zhang, X., Xu, B., Li, P., Zhang, X., Li, Z., and Zhao, Y.: Evaluating the impact of ecological construction measures on water balance in the Loess Plateau region of China within the Budyko framework, Journal of Hydrology, 601, 126596, 2021.

Zhang, L., Dawes, W., and Walker, G.: Response of mean annual evapotranspiration to vegetation changes at catchment scale, Water resources research, 37, 701-708, 2001.

Zhang, L., Hickel, K., Dawes, W., Chiew, F. H., Western, A., and Briggs, P.: A rational function approach for estimating mean annual evapotranspiration, Water resources research, 40, 2004.

Zhang, S., Yang, Y., McVicar, T. R., and Yang, D.: An analytical solution for the impact of vegetation changes on hydrological partitioning within the Budyko framework, Water Resources Research, 54, 519-537, 2018.

Zhou, G., Wei, X., Chen, X., Zhou, P., Liu, X., Xiao, Y., Sun, G., Scott, D. F., Zhou, S., and Han, L.: Global pattern for the effect of climate and land cover on water yield, Nature communications, 6, 1-9, 2015a.

Zhou, S., Yu, B., Huang, Y., and Wang, G.: The complementary relationship and generation of the Budyko functions, Geophysical Research Letters, 42, 1781-1790, 2015b.